



## Broadband higher order mode conversion using chirped microbend long period gratings

**Israelsen, Stine Møller; Rottwitt, Karsten**

*Published in:*  
Optics Express

*Link to article, DOI:*  
[10.1364/OE.24.023969](https://doi.org/10.1364/OE.24.023969)

*Publication date:*  
2016

*Document Version*  
Publisher's PDF, also known as Version of record

[Link back to DTU Orbit](#)

*Citation (APA):*  
Israelsen, S. M., & Rottwitt, K. (2016). Broadband higher order mode conversion using chirped microbend long period gratings. *Optics Express*, 24(21), 23969-23976. DOI: 10.1364/OE.24.023969

## DTU Library

Technical Information Center of Denmark

---

### General rights

Copyright and moral rights for the publications made accessible in the public portal are retained by the authors and/or other copyright owners and it is a condition of accessing publications that users recognise and abide by the legal requirements associated with these rights.

- Users may download and print one copy of any publication from the public portal for the purpose of private study or research.
- You may not further distribute the material or use it for any profit-making activity or commercial gain
- You may freely distribute the URL identifying the publication in the public portal

If you believe that this document breaches copyright please contact us providing details, and we will remove access to the work immediately and investigate your claim.

# Broadband higher order mode conversion using chirped microbend long period gratings

STINE MØLLER ISRAELSEN AND KARSTEN ROTTWITT\*

DTU Fotonik, Ørstedts Plads byg. 343, 2800 Kgs. Lyngby, Denmark

\*karo@fotonik.dtu.dk

**Abstract:** We suggest a new scheme to create chirped microbend long period gratings. Employing this scheme, the bandwidth of mode conversion between  $LP_{01}$  to  $LP_{11}$  is increased 4.8-fold with a conversion efficiency of 20 dB. This scheme includes a first time demonstration of a non-linearly chirped long period grating. The scheme is investigated both numerically using coupled mode equations as well as experimentally.

© 2016 Optical Society of America

**OCIS codes:** (050.1590) Chirping; (060.2310) Fiber optics; (060.2340) Fiber optics components.

## References and links

1. C. D. Poole, J. M. Wiesenfeld, D. J. Digiovanni, and A. M. Vengsarkar, "Optical fiber-based dispersion compensation using higher order modes near cutoff," *J. Lightwave Technol.* **12**, 1746–1758 (1994).
2. S. Ramachandran, Z. Wang, and M. Yan, "Bandwidth control of long-period grating-based mode converters in few-mode fibers," *Opt. Lett.* **27**, 698–700 (2002).
3. S. H. M. Larsen, M. E. V. Pedersen, L. Grüner-Nielsen, M. Yan, E. Monberg, P. Wisk, and K. Rottwitt, "Polarization-maintaining higher-order mode fiber module with anomalous dispersion at  $1\ \mu\text{m}$ ," *Opt. Lett.* **37**, 4170–4172 (2012).
4. L. Zhu, A. Verhoef, K. Jespersen, V. Kalashnikov, L. Grüner-Nielsen, D. Lorenc, A. Baltuška, and A. Fernández, "Generation of high fidelity 62-fs, 7-nj pulses at 1035 nm from a net normal-dispersion yb-fiber laser with anomalous dispersion higher-order-mode fiber," *Opt. Express* **21**, 16255–16262 (2013).
5. A. Verhoef, L. Zhu, S. M. Israelsen, L. Grüner-Nielsen, A. Unterhuber, W. Kautek, K. Rottwitt, A. Baltuška, and A. Fernández, "Sub-100 fs pulses from an all-polarization maintaining yb-fiber oscillator with an anomalous dispersion higher-order-mode fiber," *Opt. Express* **23**, 26139–26145 (2015).
6. S. Ramachandran, "Dispersion-tailored few-mode fibers: a versatile platform for in-fiber photonic devices," *J. Lightwave Technol.* **23**, 3426–3443 (2005).
7. V. Grubsky and J. Feinberg, "Long-period fiber gratings with variable coupling for real-time sensing applications," *Opt. Lett.* **25**, 203–205 (2000).
8. C. Poole, H. Presby, and J. Meester, "Two-mode fibre spatial-mode converter using periodic core deformation," *Electron. Lett.* **30**, 1437–1438 (1994).
9. P. Steinvurzel, K. Tantiwanichapan, M. Goto, and S. Ramachandran, "Fiber-based Bessel beams with controllable diffraction-resistant distance," *Opt. Lett.* **36**, 4671–4673 (2011).
10. Y. Kondo, K. Nouchi, T. Mitsuyui, M. Watanabe, P. G. Kazansky, and K. Hirao, "Fabrication of long-period fiber gratings by focused irradiation of infrared femtosecond laser pulses," *Opt. Lett.* **24**, 646–648 (1999).
11. D. B. Stegall and T. Erdogan, "Dispersion control with use of long-period fiber gratings," *J. Opt. Soc. Am. A* **17**, 304–312 (2000).
12. T. He, L. Rishoj, J. Demas, and S. Ramachandran, "Dispersion compensation using chirped long period gratings," *CLEO: Science and Innovations pp. STu3P-7* (2016).
13. D. Östling and H. E. Engan, "Broadband spatial mode conversion by chirped fiber bending," *Opt. Lett.* **21**, 192–194 (1996).
14. S. Ramachandran, J. Wagener, R. Espindola, and T. A. Strasser, "Effects of chirp in long period gratings," *Bragg Gratings, Photosensitivity, and Poling in Glass Waveguides p. BE1* (1999).
15. L. Grüner-Nielsen and J. W. Nicholson, "Stable mode converter for conversion between  $LP_{01}$  and  $LP_{11}$  using a thermally induced long period grating," *Proceedings of IEEE Summer Topical Meeting pp. 214–215* (2012).
16. R. C. Youngquist, J. L. Brooks, and H. J. Shaw, "Two-mode fiber modal coupler," *Opt. Lett.* **9**, 177–179 (1984).
17. R. Kashyap, *Fiber Bragg Gratings* (Academic press, 1999).
18. X. Shu, L. Zhang, and I. Bennion, "Fabrication and characterisation of ultra-long-period fibre gratings," *Opt. Commun.* **203**, 277–281 (2002).
19. A. M. Vengsarkar, P. J. Lemaire, J. B. Judkins, V. Bhatia, T. Erdogan, and J. E. Sipe, "Long-period fiber gratings as band-rejection filters," *J. Lightwave Technol.* **14**, 58–65 (1996).

## 1. Introduction

Broadband mode conversion have several applications e.g. within group velocity dispersion (GVD) compensation [1–3] which may be used in ultrashort pulsed lasers [4,5], but also within sensing [6]. The ability to achieve a broader and tailorable conversion bandwidth is thus highly desirable. This is possible either by engineering the fiber and using the point where the group delay difference between the two modes in the conversion process is zero [1–3,7] or as we demonstrate in this work using a chirped long period (LPG). LPGs have been demonstrated in many forms including microbend [1], CO<sub>2</sub>-formed [8], UV-induced [2,9] and formed using high intensity light [10]. Chirped LPGs are more versatile in the way that we only need to design the chirp of the LPG to achieve broadband conversion and the method is thus in principle applicable to all fibers. It has also been showed that chirped LPGs have a GVD compensating effect by them selves. This has been demonstrated both theoretically [11] and recently also experimentally [12]. However, in this work, we focus on broadband mode conversion. Chirped fiber LPGs for broadband mode conversion was first suggested by Östling *et al.* [13]. The scheme presented in this work elaborates the idea presented by Östling and shows a straight forward way to implement linear and nonlinear chirp in a microbend LPG. Note that employing a microbend LPG limits the mode conversion to conversion between symmetric and anti-symmetric modes [1]. Chirping have also been demonstrated for UV-induced LPGs [12,14] which allows for coupling to symmetric modes.

The principle of implementation of chirped microbend LPGs is outlined in Fig. 1.

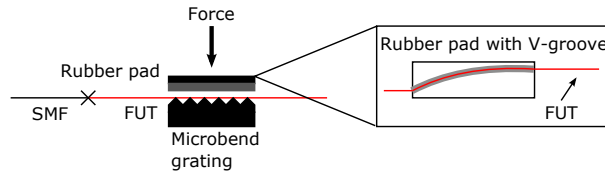


Fig. 1. Principle of the chirped microbend LPG. The fiber under test (FUT) is perturbed by a microbend LPG. The chirp in the LPG is made by a curved groove in the rubberpad used to press the fiber onto microbend LPG.

We employ microbend LPGs as higher order mode converters. However, instead of holding the fiber under test (FUT) straight as is customary [15], the FUT is curved upon the microbend LPG. The curve is achieved by placing the FUT in a groove in the rubber pad pressing the FUT onto the microbend LPG. The groove feature enables a simple and versatile tool for tailoring the chirp of the LPG; the shape of the groove simply defines the chirp.

Initially, the mode conversion is considered numerically. Östling *et al.* limit their investigation to linearly chirped microbend LPGs [13]. Here we also consider nonlinearly chirped LPGs. This is to our knowledge the first demonstration of nonlinearly chirped LPGs.

We use coupled mode theory to simulate the conversion efficiency of the chirped microbend LPG [13]. If  $a_{01}$  and  $a_{11}$  are the complex modal amplitudes of LP<sub>01</sub> and LP<sub>11</sub>, respectively, and  $\kappa$  is the coupling coefficient, then

$$\begin{aligned} \frac{da_{01}}{dz} &= -i\kappa a_{11} \exp\left(i \int_0^z \Delta\beta(\lambda, x) dx\right) \\ \frac{da_{11}}{dz} &= -i\kappa^* a_{01} \exp\left(-i \int_0^z \Delta\beta(\lambda, x) dx\right), \end{aligned} \quad (1)$$

where

$$\Delta\beta(\lambda, z) = 2\pi[1/L_B(\lambda) - 1/\Lambda(z)], \quad (2)$$

where  $L_B(\lambda)$  is the measurable beat length between the two modes and  $\Lambda(z)$  is the pitch of the LPG [16]. The pitch of the LPG in the fiber may be described as  $\Lambda(z) = \Lambda_0 + \delta(z)$ , where  $\Lambda$  is the unperturbed pitch of the LPG while the perturbation,  $\delta(z)$ , describes the linear or nonlinear chirp.  $\kappa$  is the coupling coefficient proportional to the force applied to the rubber pad;  $\kappa$  is assumed constant along  $z$ . Changing  $\kappa$  along  $z$  would be beneficial in the design of LPG spectra for example when reducing the number of sidebands for GVD compensation [12]. However, this is difficult to implement in this scheme as it requires very high precision in the design of the rubber pad thickness as well as knowledge of the material properties of the used rubber. The coupled mode equations are solved numerically employing an ODE solver, as Eq. 1 does not yield a physically intuitive closed form solution [14].

To achieve the widest conversion bandwidth, we employ a nonlinearly chirped LPG with pitch in form of a 2nd order polynomial. To find the set of coupled differential equations to implement in the ODE solver, the integral

$$\begin{aligned} \int_0^z \Delta\beta(\lambda, x) dx &= \int_0^z 2\pi \left( \frac{1}{L_B(\lambda)} - \frac{1}{\Lambda(x)} \right) dx \\ &= \int_0^z 2\pi \left( \frac{1}{L_B(\lambda)} - \frac{1}{ax^2 + bx + c} \right) dx \end{aligned} \quad (3)$$

is solved.

## 2. Numerical investigations

We consider a TrueWave fiber operated at 800 nm, where it is fewmoded and guides  $LP_{01}$  and  $LP_{11}$ . We want to couple from  $LP_{01}$  to  $LP_{11}$ . We employ a higher order diffraction LPG to achieve phase matching [17]. The first order diffraction is not achievable due to a mechanical constraint: For pitches comparable to the fiber diameter (that is including the coating), the mechanical grating is not able to bend and perturb the fiber.

To find the fitting parameters of the chirp, the beat length within the desired wavelength range is approximated with a second order polynomial using the longitudinal axis of the LPG as the independent variable of the fit. The second order polynomial is used in accordance with Eq. 3. The aim is to achieve broadband conversion without overcoupling around 800 nm and the optimization of the chirp parameters is limited to the lower wavelength limit of the beat length measurement and the turn-around-point around 870 nm [7].

In Fig. 2(a), the full measurement of the beat length is plotted. The phase matching curves are measured exciting the  $LP_{11}$ -mode at variable pitches and registering the resonances. The multiple curves are a result of the higher order diffraction and their sidebands. The higher order diffraction curves are marked with a red line corresponding to the fit in Fig. 2(b) scaled to the diffraction order. The remaining points are sidebands. Sidebands have previously been observed using higher order diffraction [18]. The first order diffraction is not achievable as previously explained. The phase matching measurement corresponding to second order diffraction is plotted in Fig. 2(b), the order of the diffraction is identified from the full phase matching measurement in Fig. 2(a). The phase matching measurement is fitted to a fourth order polynomial. In Fig. 3 the transmission, that is the remaining power in the fundamental mode after the LPG, is plotted as function of the wavelength and coupling coefficient for an unchirped LPG with a  $\Lambda = 525 \mu\text{m}$  which corresponds to conversion at 800 nm employing second order diffraction. -20 dB transmission is achieved with a 1.8 nm bandwidth without overcoupling, that corresponds to the lowest coupling coefficient  $\kappa$  that allows for -20 dB transmission. The transmission is found

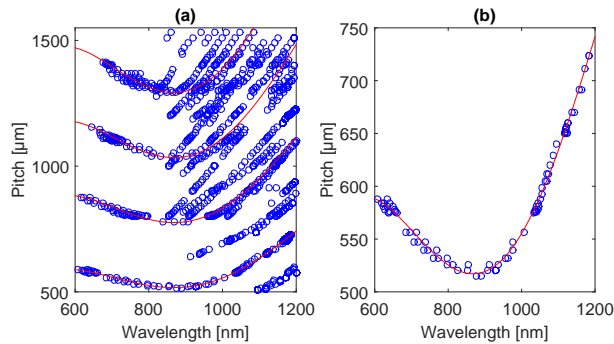


Fig. 2. Phase matching curves for the conversion of  $LP_{01}$  to  $LP_{11}$  in a TrueWave<sup>®</sup> fiber operated in a fewmoded regime. (a) Full measurement of phase matching curves for higher order conversions corresponding to  $\Lambda = 2L_B$ ,  $\Lambda = 3L_B$ ,  $\Lambda = 4L_B$ , and  $\Lambda = 5L_B$ . The red lines in the plot correspond to 4th order polynomial fit in (b) scaled to the order of conversion. (b) Selected data for the pitch corresponding to  $\Lambda = 2L_B$ . The data is fitted to 4th order polynomial.

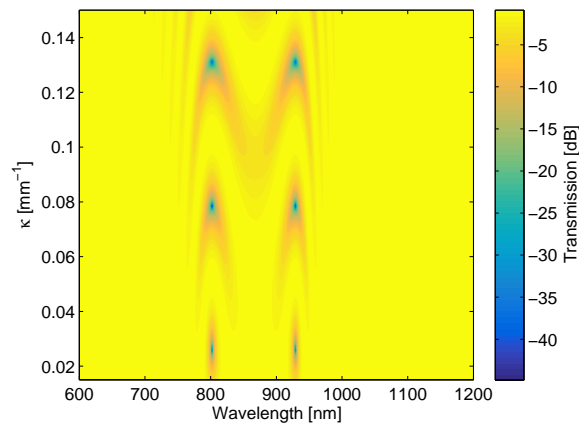


Fig. 3. Numerically generated transmission data for the conversion of  $LP_{01}$  to  $LP_{11}$  in a TrueWave fiber operated in a fewmoded regime. The applied mode converter is an unchirped LPG with a pitch of  $525 \mu\text{m}$  which corresponds to conversion at  $800 \text{ nm}$ .

using a numerical implementation of the coupled mode theory as described in Eq. 1. The transmission of a nonlinearly chirped LPG optimized for broadband conversion around  $800 \text{ nm}$  is plotted in Fig. 4 as a function of the wavelength and the coupling coefficient. To perform the optimization of the chirp, the measured beat length within the desired wavelength range is approximated with a second order polynomial using the longitudinal axis of the LPG as the independent variable of the fit. The second order polynomial is used in accordance with 3. With a  $-20 \text{ dB}$  transmission across a  $8.6 \text{ nm}$  bandwidth, a 4.8-fold increase of the bandwidth is achieved. As for the unchirped LPG, the transmission is found using a numerical implementation of the coupled mode theory as described in 1 with the condition of 3. Note that the conversion to  $LP_{11}$  is achieved for higher values of the coupling coefficient,  $\kappa$ , corresponding to a larger force upon the rubber pad, hence there is a trade off between conversion bandwidth and possible permanent mechanical deformation of the fiber due to the larger load.

For closer examination, the transmission of the microbend LPGs in the chirped and unchirped

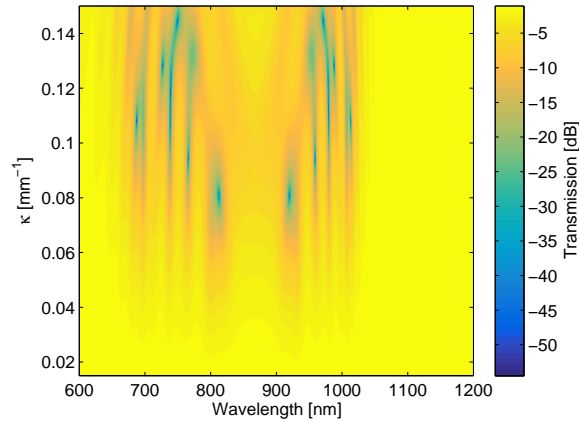


Fig. 4. Numerically generated transmission data for the conversion of  $LP_{01}$  to  $LP_{11}$  in a TrueWave fiber operated in a fewmoded regime. The applied mode converter is a nonlinearly chirped LPG where the chirp is optimized for conversion around 800 nm.

configuration is plotted in Fig. 5 applying the coupling coefficient  $\kappa$  yielding the largest dip in transmission without overcoupling. In this figure, it is evident that the chirped LPG has a significantly broader bandwidth, if we consider the 3 dB bandwidth there is an 23-fold increment. However with coupling coefficients of  $0.026 \text{ mm}^{-1}$  and  $0.081 \text{ mm}^{-1}$  for the unchirped and chirped configuration, respectively, the risk of permanent deformation of the fiber is much larger for the chirped LPG.

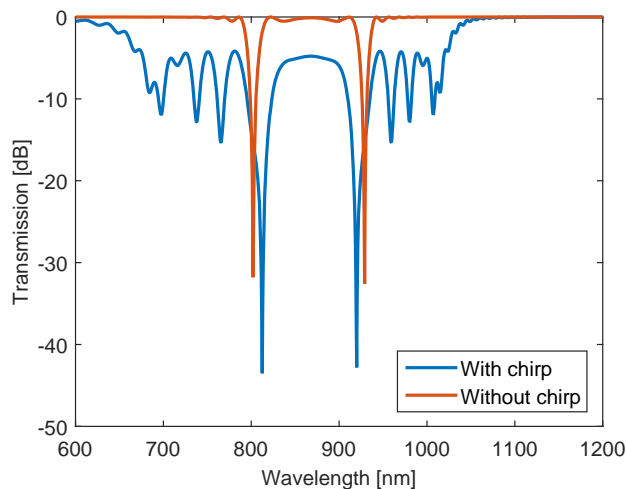


Fig. 5. Numerically determined transmission plot of the chirped and the unchirped LPG. For the chirped LPG, a coupling coefficient of  $0.08115 \text{ mm}^{-1}$  is applied and for the unchirped LPG, a coupling coefficient of  $0.0258 \text{ mm}^{-1}$ .

### 3. Experimental investigations

For the experimental investigations, the shape of the V-groove must be designed according desired nonlinear chirp as the one used in the numerical investigations. Thus the parametric curve describing the chirp,  $\mathbf{r}(u)$  is written as

$$\oint_L = \int_0^z |\mathbf{r}'(u)| du = \Lambda(z) \quad (4)$$

Thus the line integral along the V-groove is equal to the pitch as function of  $z$ . This is however not easily solved. Instead, we approximate with a piecewise linear function, the pieces correspond to each step as the rubberpad is pressed on to the alumina block creating the microbends. To carve a smooth curve in the rubberpad, the piecewise linear function is approximated with a third order polynomial.

In this section, a physical realization of the setup in Fig. 1 is considered. We consider the results of an experimental realization of the nonlinearly chirped LPG. The chirp is tailored to the phase matching curve as for the numerical calculation in Fig. 4. The transmission is measured by launching a broadband source in to the fundamental mode of the FUT as illustrated in Fig. 1 and after the chirped microbend LPG the FUT is spliced to a single mode fiber (@ 800 nm). This is a standard method for characterizing the conversion of LPG to the higher order mode [19]. Secondly, the transmission plot shows very little multipath interference indicating excitation of a single mode by the LPG, which verifies the assumption of no other losses in the transmission measurement. The transmission is measured as function of the translation of the stage controlling the position of the rubber pad. Note, that the force on the rubber pad increase with a decreasing value of the translation. In principle, the translation of the rubber pad is linearly proportional to the force on the rubber pad and thereby the coupling coefficient,  $\kappa$ , but due to mechanical restraints of the setup and the mechanical properties of the rubber pad, the relation between translation and force is not complete linear.

Initially, we measure a reference given by a nonchirped microbend LPG tailored for conversion at 800 nm corresponding to pitch of 525nm. The transmission mapping as function of the translation of the rubber pad is plotted in Fig. 6.

Transmission as function of the wavelength and the translation of the stage, i.e. the coupling coefficient,  $\kappa$ , for the nonlinearly chirped LPG applying second order diffraction tailored for conversion at 800 nm using the measured phase matching curves plotted in Fig. 2 is plotted in Fig. 7. In both the transmission wavelength spectra of the chirped and the unchirped LPG, there are some features around 1050 nm independently of the translation, which is a result of unstable excitation source and not the microbend LPGs.

In the experimental transmission spectra of the nonlinearly chirped LPG, we observe many of the same features as we see in the numerical results. Unfortunately, we are not able to map some of the high conversion efficiency effects. That is a result of the use of second order diffraction in the LPG demanding higher values of the coupling coefficient than first order diffraction and the mechanical constraint of a microbend LPG limiting the conversion to HOMs to what is possible without permanently damaging or potentially breaking the fiber. The linearity between the plotted translation and the coupling coefficient is also limited by the relaxation of the microbend LPG as described by G.-Nielsen *et al.* [15]. However, as we employ a rubber pad the relaxation is reduced.

In Fig. 8, the best possible conversion for the chirped and the unchirped LPG in the True-Wave fiber is plotted. In both the numerical and experimental studies, the chirped LPG requires a higher coupling coefficient,  $\kappa$ , - given by the translation of the rubber pad - for optimum coupling. There are several features to notice in this plot: The first is that the transmission plot for the unchirped LPG does not only show one dip as the simulations. We expect that this is a result



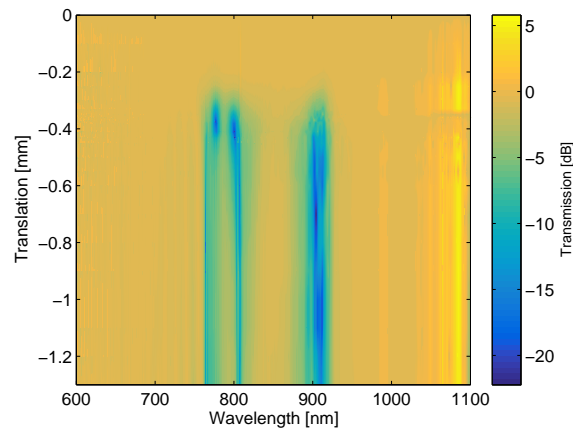


Fig. 6. Experimental transmission data for the conversion of  $LP_{01}$  to  $LP_{11}$  in a TrueWave fiber operated in a fewmoded regime. The coupling coefficient is given by the translation of the rubber pad given by the translation of the stage controlling the position of the rubber band. The applied mode converter is an unchirped LPG with a pitch of  $525 \mu\text{m}$  which corresponds to conversion at 800 nm.

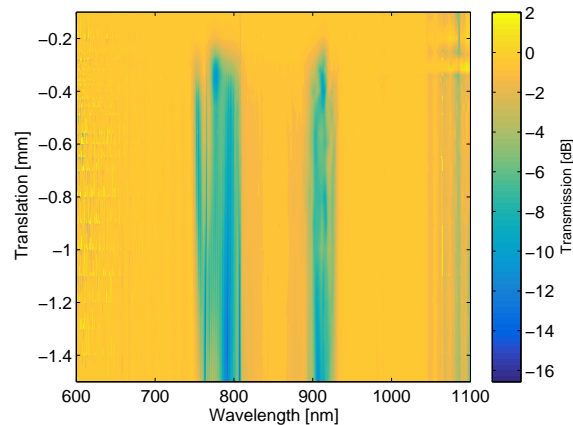


Fig. 7. Experimental transmission data for the conversion from  $LP_{01}$  to  $LP_{11}$  in a TrueWave fiber operated in a fewmoded regime. The coupling coefficient is given by the translation of the rubber pad given in the translation of the stage controlling the position of the rubber band. The applied mode converter is a nonlinearly chirped LPG where the chirp is optimized for conversion around 800 nm.

of the second order diffraction used. The second is the squareness of the transmission spectrum for the chirped LPG, a feature which has been achieved without overcoupling and unwanted spectral oscillatory behavior [14]. This feature is very attractive for GVD compensation using chirped LPGs [11, 12]. There is no significant broadening in the chirped LPG if we consider both dips in the transmission spectrum close to 800 nm for the unchirped LPG. However, we recall that the chirp was designed only for the dip at 800 nm. Using this fact, the conversion bandwidth is enhanced 2.7-fold at 5 dB conversion. Due to mechanical constraints of this system, it is unfortunately not possible to achieve higher values of the coupling coefficient for this



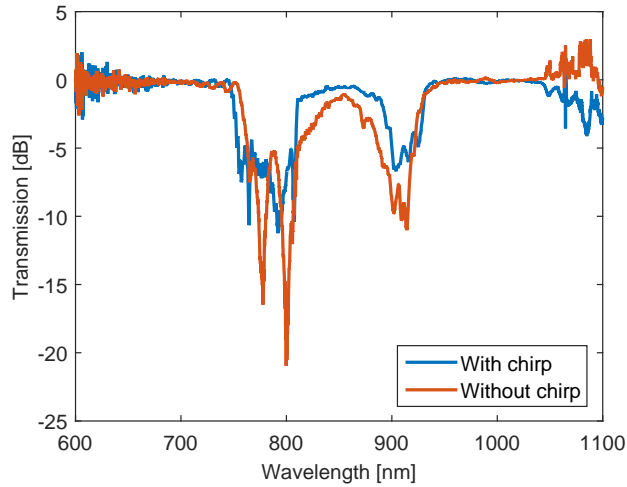


Fig. 8. Measured transmission plot of the chirped and the unchirped LPG in the TW fiber. For the chirped LPG, a translation of -0.41 mm is used and for the unchirped LPG, a translation of -1 mm is used.

system, which would most likely have resulted in larger conversion. There is increased need for the high conversion efficiencies in this system due to the use of higher order diffraction.

#### 4. Summary

In summary, we have demonstrated a new and versatile platform for chirped LPGs coupling from a symmetrical to an anti-symmetrical mode and vice versa. The transmission characteristics of this scheme has been modelled using coupled mode theory and a 4.8-fold increase of the bandwidth is achieved for conversion from  $LP_{01}$  to  $LP_{11}$  in a TrueWave fiber operated in a fewmoded regime.